INTERNATIONAL ATOMIC ENERGY AGENCY
UNITED NATIONS EDUCATIONAL, SCIENTIFIC AND CULTURAL ORGANIZATION
INTERNATIONAL CENTRE FOR THEORETICAL PHYSICS
I.C.T.P., P.O. BOX 586, 34100 TRIESTE, ITALY, CABLE CENTRATOM TRIESTE

H4.SMR/845-6

Second Winter College on Optics

20 February - 10 March 1995

Light Scattering by Tissues

G. Zaccanti

University of Florence
Department of Physics
Florence, Italy

Photon migration through biological tissues

Giovanni Zaccanti
Università di Firenze, Dipartimento di Fisica, Sezione di Fisica Superiore,
Via Santa Marta 3, 50139, Firenze, Italy

These lessons mainly concern with light propagation through scattering media. The aim is to give basic concepts governing light propagation through biological tissues in order to understand what kind of information may be obtained on biological tissues by using light as a probe.

Many techniques are currently available to obtain imaging and functional monitoring of biological tissues:
x-ray
NMR
EPR
Ultrasounds
etc.

It is well known that a lot useful information may be obtained by using these techniques. As an example, x-rays have given the first opportunity "to see" inside the human body. Biological tissues are relatively transparent to x-ray and an image can be obtained by the "shadow" produced by the tissue "illuminated" by a collimated x-ray source. Different tissues differently absorb x-rays: in particular, bones absorb more than soft tissues, thus it is simple to "see" bones with this technique.
However, by using x-rays it is difficult to obtain information on soft tissues because there are small differences between different soft tissues in absorbing x-rays. Further, x-rays cannot distinguish between living and dead tissues. Therefore these techniques are not useful to monitor the status of living tissues.
Another limitation in using x-rays is the damage that they can produce on tissues: as an example, x-rays used for mammography are suspected to induce about 0.5% of breast tumors. Therefore this technique is not usable for frequent controls as desirable for screening.

Although a lot of useful information can be obtained by using currently available techniques, there is still a strong request for new techniques, possibly non invasive, for imaging and monitoring living tissues.

Light gives a unique probe to study living tissues. It is very simple to distinguish between living and dead tissues, or to have first information on the health of the tissue, looking at the "color" of the tissue. At visible and near infrared wavelengths light propagation is strongly influenced by many cromophores present inside the biological tissue that are related to the health status of the tissue. As an example, we know that venous and arterial blood have a different colour due to the different degree of blood oxygenation. Therefore we can understand that very useful information on the status of the tissue, like the blood oxygen saturation, can be obtained measuring the "color" of the tissue.

A lot of information useful for the doctor can thus be obtained if we can properly measure the optical properties of the tissue.

There is thus a big potential to obtain basic information on tissues by using radiation in the visible and near infrared region of the electromagnetic spectrum, but there are relatively little currently available instrumentation based on light. The reason is that measurements of optical properties of tissues are difficult. Recent progress on optoelectronics, especially the availability of light sources emitting ultrashort pulses (picosecond lasers) and ultrafast detectors (streak camera, microchannel plate), aroused the concern for developing new instrumentation and provoked an impressive interest of researchers and industries for developing tissue optics.

Thus we will introduce optical properties of biological tissues and the physical laws governing light propagation in order to understand what kind of information can be obtained from optical measurements and the difficulties related to these measurements.

Biological tissues are highly diffusing media. We thus begin:
1) To introduce the optical parameters used to characterize diffusing media,
2) To introduce the radiative transfer equation governing photon migration;
3) To briefly describe theories and methods currently used for studying tissue optics;
4) To describe in particular the Monte Carlo method and to illustrate a code developed to visualize photon migration;
5) To describe different techniques currently studied for imaging and monitoring of biological tissues.

PARAMETERS USED TO DESCRIBE THE OPTICAL PROPERTIES OF DIFFUSING MEDIA

Optical properties of a single diffusing particle

The energy of a plane wave impinging on a (small) particle having dielectric properties different from the surrounding medium is partially absorbed and scattered.

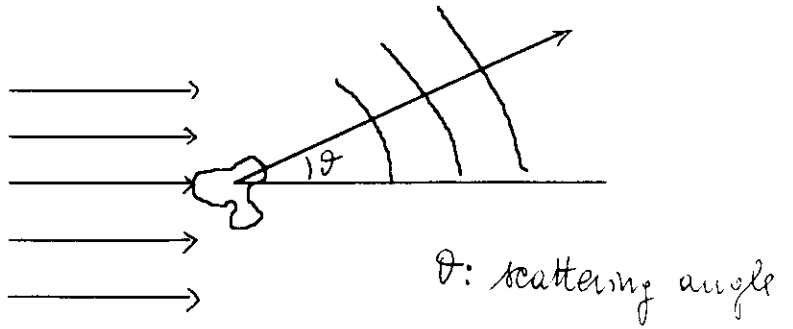

When unpolarized radiation is considered, the scattering and absorption properties are described by:

C_s= scattering cross section = (total scattered power)/(intensity of the incident wave) $[mm^2]$

C_a = absorption cross section = (absorbed power)/(intensity of the incident wave) $[mm^2]$

$C_{ext} = C_a + C_s$ = extinction cross section = (total scattered + absorbed power)/(intensity of the incident wave) $[mm^2]$

We can interpret the cross section as the equivalent area of a hypothetical perfectly absorbing disk on the path between source and detector producing the same attenuation on propagation.

$p(\vartheta)$ (scalar) scattering (or phase) function: describes the angular distribution of scattered light. Represents the probability that the radiation is scattered, per unit solid angle, with a scattering angle ϑ.

It is also useful to define:

$Q_s = C_s / C_g$ scattering efficiency

$Q_a = C_a / C_g$ absorption efficiency

$Q_{ext} = C_{ext} / C_g$ extinction efficiency

with C_g geometrical cross section of the particle

The scattering properties strongly depend on the size parameter, x, of the particle and on the refractive index. For spherical particles $x = 2\pi a / \lambda$ (with a = radius of the particle, λ = wavelength)

As an example, the following figures report Q_s versus the asymmetry factor x and the scattering functions referring to different sizes of spheres. Data refers to polystyrene spheres suspended in water (relative refractive index 1.20) at the He-Ne wavelength (633 nm).

M. Kerker, "The scattering of Light—" Academic Press (1969)

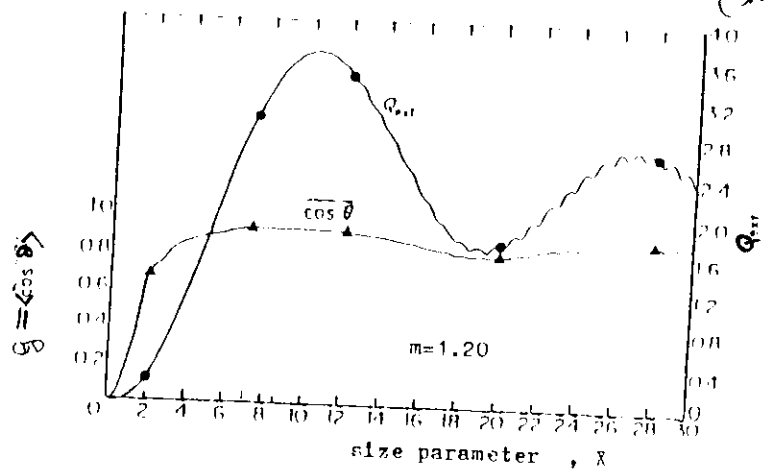

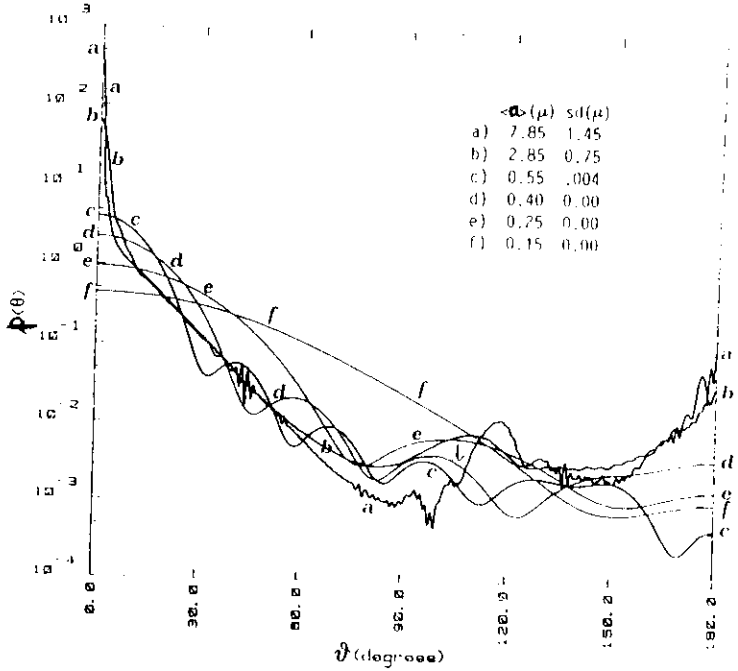

For small particles ($a \ll \lambda$, Rayleigh scattering), the scattering function is more or less isotropic and Q_s is proportional to x^4. For large particles ($a \gg 10\lambda$) $Q_s \approx 2$ and $p(\vartheta)$ becomes more and more forward peaked when x increases. For spherical particles the scattering properties can be evaluated by using Mie theory.

Optical properties of a collection of randomly distributed diffusing particles

For a collection of particles with low concentration (distance between particles sufficiently large with respect to the wavelength) and randomly distributed, interference effects between energy scattered by different particles can be neglected and the energy scattered by different particles can be simply added. The optical properties of a collection of particles is thus described by:

μ_s= scattering coefficient = (total power scattered by particles per unit volume)/(intensity of the incident wave) $[mm^{-1}]$

μ_a = absorption coefficient = (total power absorbed by particles per unit volume)/(intensity of the incident wave) $[mm^{-1}]$

$\mu_{ext} = \mu_a + \mu_s$ = extinction coefficient = (total scattered + absorbed power extracted by particles per unit volume)/(intensity of the incident wave) $[mm^{-1}]$

For a monodispersion of particles: $\mu_s = n C_s$ (with $n\left[mm^{-3}\right]$ = particles per unit volume and C = cross section) and the scattering function of the single particle also describes the angular distribution of energy scattered by a volume element.

For a monodispersion of spherical particles with volume concentration ρ,

$n = \rho / (\frac{4}{3}\pi a^3)$ and

$$\mu_s = n Q_s(a) \pi a^2 = \frac{4}{3}\frac{\rho}{a} Q_s(a)$$

For a fixed volume concentration of diffusers the extinction coefficient strongly depends on the size of the diffusers. As an example, the figure reports μ_s versus a for a suspension of particles having a volume concentration of 1%. The extinction coefficient is maximum when $a \approx \lambda$.

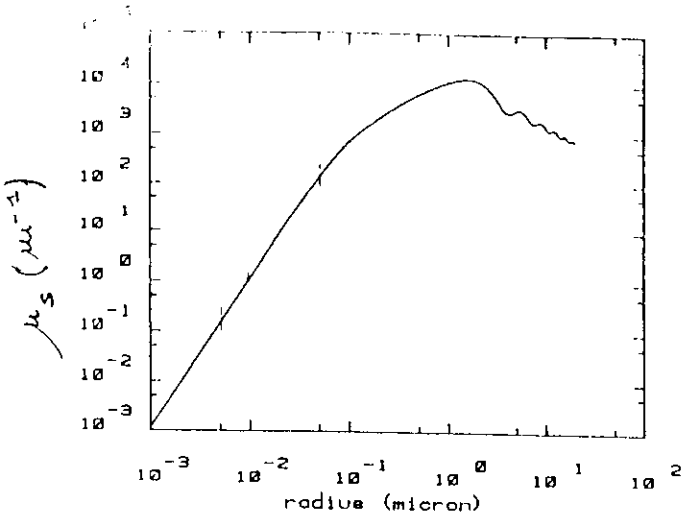

Extinction coefficient for a monodispersion of spheres ($n = 1.20$). $\lambda = 633 nm$

Particle concentrat. 1%

For a polydispersion of particles μ and $p(\vartheta)$ are obtained averaging on the particle distribution the diffusing properties of single particles.

It is also useful to define:

$$w_0 = \frac{\mu_s}{\mu_s + \mu_a} = \text{single scattering albedo}$$

$$g = \langle \cos(\vartheta) \rangle = \int_{4\pi} \cos(\vartheta) p(\vartheta) d\Omega \quad \text{asymmetry factor}$$

ATTENUATION OF A COLLIMATED BEAM PROPAGATING THROUGH A DIFFUSING MEDIUM

The attenuation of a collimated beam propagating through a diffusing medium is described by the Lambert-Beer law.

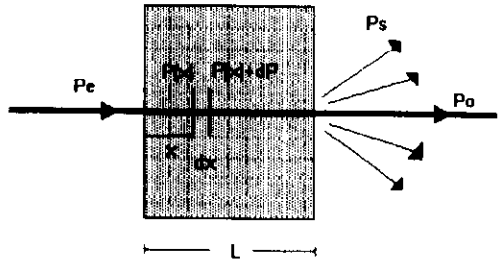

$dP = -\mu_{ext} P(x) dx$ and thus: $P(x) = P_c \exp(-\mu_{ext} x)$. The unscattered component of the power transmitted through a homogeneous slab of thickness L is given by:

$$P_0 = P_c \exp(-\tau_{ext}) \qquad \text{Lambert-Beer law}$$

with:

$$\tau_{ext} = \mu_{ext} L = \ln \frac{P_c}{P_0} \qquad \text{optical depth}$$

The extinction coefficient can obtained measuring the attenuation of the unscattered beam by means of a transmissometric apparatus.

Statistical interpretation of optical coefficients

We have seen that the scattering function describes the probability for the photon to be scattered in different directions. We can see that also the scattering (absorption, extinction) coefficient has a simple statistical interpretation
Indicating with p(r) the probability density function to have scattering at a distance r from the source for photons migrating through a non-absorbing medium, we have:

$$p(r)dr = dP / P_c = \mu_s \exp(-\mu_s r) dr$$

and thus:

$$p(r) = \mu_s \exp(-\mu_s r)$$

from which the mean free path between two subsequent scattering events follows:

$$\langle r \rangle = \int_0^\infty r\, p(r)\, dr = \frac{1}{\mu_s}$$

Similar relationships can be derived for μ_a and μ_{ext}.

The mean free path is the "natural" unit to measure lengths when we study photon migration through diffusing media. The length measured by using this unit, i.e., the product $r\mu$, is the optical length.

Scaling rule: a detector measuring photons received from a source after migration through two diffusing media having different μ_{ext} and 1) the same scattering function, 2) the same single scattering albedo, and 3) scaled geometrical dimensions,

measures the same energy in the two cases if the optical distances are the same, i.e., if the product between μ_{ext} and the geometrical distances remains unchanged.

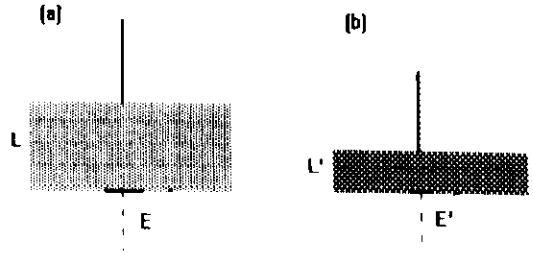

$$\mu L = \mu' L' \longrightarrow E = E'$$

It is possible to demonstrate that for an infinitely extended non-absorbing medium, for photons emitted along the z axis by a source placed at z = 0 we have, after k scattering events:

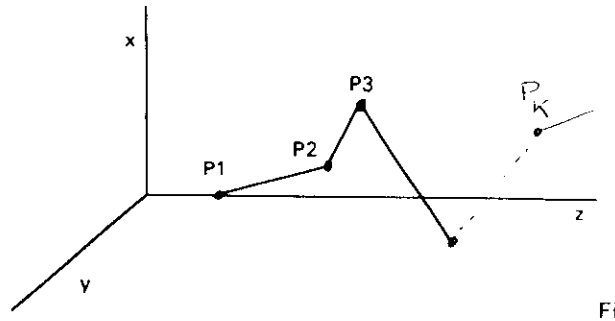

Fig.

$$\langle x_k \rangle = \langle y_k \rangle = 0 \quad \text{and}$$

$$\langle z_k \rangle = \frac{1}{\mu_s}\left(1 + \sum_{i=1}^{k-1} g^i\right)$$

and for large values of k:

$$\lim_{k \to \infty} \langle z_k \rangle = \frac{1}{\mu_s} \frac{1}{1-g}$$

The quantity $\frac{1}{\mu_s}\frac{1}{1-g}$ represents the mean distance followed by photons along the original direction of motion before they "forget" the original direction.

The quantity:

$\mu_s' = \mu_s(1-g)$

is the reduced scattering (or transport) coefficient and practically fully describes the scattering properties of the medium when propagation through thick diffusing media (like tissues) is considered.

We also can demonstrate that the mean square distance of photons after k orders of scattering is given by:

$$<d_k^2> = <x_k^2 + y_k^2 + z_k^2> = 2\frac{k(1-g) - g + g^{k+1}}{\mu_s'^2}$$

and for large values of k (the asymmetry factor g is g<1):

$$<d_k^2> \approx 2\frac{k(1-g)}{\mu_s'^2}$$

Similarity rule

Photons migrating through two different highly diffusing media, in the same geometrical condition, having different scattering properties (different values for μ_s and $p(\vartheta)$), but with the same value for the reduced scattering coefficient μ_s', are expected to have "similar" spatial distributions, even if the number of scattering events involved in photon migration may be very different. As an example, photons migrating through a medium having the asymmetry factor g are expected, after k scattering events, to have the same value for $<d_k^2>$ and $<z_k>$ like photons migrating through a medium having g=0 (isotropic scattering) after k_0 scattering events, with: $k_0 = k(1-g)$. Comparing the spread of photons after k and k_0 scattering events we thus expect to have "similar" spatial distributions.

The optical parameters μ_s' and μ_a are thus sufficient to describe photon migration through media with high optical thickness. Therefore the "natural" unit for measuring lengths becomes $1/\mu_s'$ (diffusion length or reduced scattering length), representing the mean distance followed by photons before "forgetting" the original direction of motion. It is thus useful to introduce also the reduced scattering optical thickness $\tau_s' = L\mu_s'$.

Whereas the scaling rule previously presented is rigorous, (it is possible to demonstrate this rule as a property of the radiative transfer equation describing photon migration through turbid media) the similarity rule presented is only approximated since it comes from approximated relationships that are fulfilled only after a sufficiently large number of scattering events. The similarity rule is thus applicable only to propagation through media having a sufficiently high reduced scattering optical thickness.

Theories used to describe photon migration through biological tissues

Radiative transfer equation

Photon migration through diffusing media is described by the radiative transfer equation:

$$\left\{\hat{s}\cdot\nabla + \mu_a + \mu_s + \frac{1}{v}\frac{\partial}{\partial t}\right\}\Phi(\vec{r},\hat{s},t) = q(\vec{r},\hat{s},t) + \mu_s \int_{4\pi} p(\hat{s},\hat{s}')\Phi(\vec{r},\hat{s}',t)d^2\hat{s}'$$

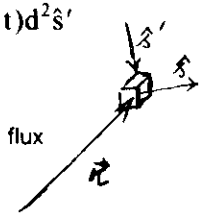

where:

$\Phi(\vec{r},\hat{s},t)$ $\left[Wm^{-2}sr^{-1}\right]$ is the radiance, i.e., the average power flux density at $\vec{r}$ in the direction $\hat{s}$ at time t within a unit solid angle;

$q(\vec{r},\hat{s},t)$ is the source term;

$p(\hat{s},\hat{s}')$ is the scattering function.

The term: $\hat{s}\cdot\nabla\Phi(\vec{r},\hat{s},t)$ (also written as $d\Phi(\vec{r},\hat{s},t)/d\hat{s}$) represents the change in radiance in the $\hat{s}$ direction. The term $(\mu_a+\mu_s)\Phi(\vec{r},\hat{s},t)$ represents the decreasing of radiation due to absorbtion and scattering; $\frac{1}{v}\frac{\partial}{\partial t}\Phi(\vec{r},\hat{s},t)$ represents the temporal variation and $\mu_s\int_{4\pi} p(\hat{s},\hat{s}')\Phi(\vec{r},\hat{s}',t)d^2\hat{s}'$ the total amount of radiation scattered into the direction $\hat{s}$ from all directions.

There are not general solutions to solve the radiative transfer equation, but only approximated analytical theories and numerical methods. We will describe in particular the Monte Carlo technique.

Analytical models:

Diffusion approximation: Is obtained by considering the lowest order approximation of the expansion in spherical harmonics of the radiative transfer equation:

$$\left\{\nabla\cdot(D(\vec{r})\nabla) - \mu_a - \frac{1}{c}\frac{\partial}{\partial t}\right\}\tilde{\Phi}(\vec{r},t) = -q_0(\vec{r},t)$$

where:

$\tilde{\Phi}(\vec{r},t) = \int_{4\pi}\Phi(\vec{r},\hat{s},t)d^2\hat{s}$ is the irradiance (or fluence rate);

$q_0(\vec{r},t)$ is an isotropic source term

and $D(\vec{r})$ is the diffusion coefficient. Almost in all literature the following expression:

$$D(\vec{r}) = \frac{1}{3(\mu_a+\mu_s(1-g))}$$

is assumed for the diffusion coefficient. However, in a recent paper Furutzu and Yamada, (Phys. Rev. E, 50, pp.3634,1994), demonstrated that the correct dependence of $D(\vec{r})$ is:

$$D(\vec{r}) = \frac{1}{3\mu_s(1-g)}$$

i.e., independent of μ_a.

The diffusion equation has been solved for homogeneous diffusing media for different boundary conditions (infinitely extended medium, semi-infinite slab, finite slab, cylinder, sphere). The solutions obtained well describe photon migration when $\mu_s' >> \mu_a$ and $\tau_s' = \rho\mu_s' > 10$, i.e., when the distance ρ of the detector from the source is larger than about 10 diffusion lengths.

For a slab (thickness L) Patterson et al. (Appl. Opt. Vol. 28, pp.2331, 1989) obtained the following relationships for the time resolved reflectance $(R(\rho,L,t))$ and transmittance $(T(\rho,L,t))$:

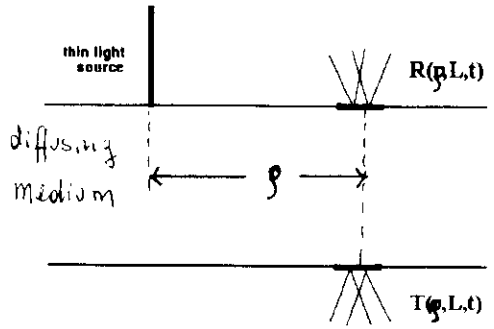

$$R(\rho,L,t) = (4\pi Dc)^{-3/2} t^{-5/2} \exp(-\mu_a ct) \exp(-\frac{\rho^2}{4Dct})$$
$$* \left\{ z_o \exp(-\frac{z_o^2}{4Dct}) - (2L - z_o) \exp(-\frac{(2L - z_o)^2}{4Dct}) \right.$$
$$\left. + (2L + z_o) \exp(-\frac{(2L + z_o)^2}{4Dct}) \right\}$$

$$T(\rho,L,t) = (4\pi Dc)^{-3/2} t^{-5/2} \exp(-\mu_a ct) \exp(-\frac{\rho^2}{4Dct})$$
$$* \left\{ (L - z_o) \exp(-\frac{(L - z_o)^2}{4Dct}) - (L + z_o) \exp(-\frac{(L + z_o)^2}{4Dct}) \right.$$
$$\left. + (3L - z_o) \exp(-\frac{(3L - z_o)^2}{4Dct}) - (3L + z_o) \exp(-\frac{(3L + z_o)^2}{4Dct}) \right\}$$

where $z_o = 1/\mu_s'$ and ρ is the distance of the detector from the thin light beam.

Random walk: the motion of a photon in the scattering medium is approximated as a "random walk" on a simple cubic lattice (whose size is related to $1/\mu_s'$): the photon proceeds through the lattice as steps to one of six nearest neighboring lattice points.

By using this simple scheme it is possible, for homogeneous media, to obtain analytical relationships similar to the ones obtained by using the diffusion approximation.

Numerical methods:
Finite Element Method (FEM) :FEM is a classic technique to solve differential equations. The FEM considers a grid of discrete points on the variables domain (space and time) and the continuous function of these variables is replaced by a discrete function which samples the continuous function at the grid points. This method is very useful to study problems with complex boundary conditions and non homogeneous optical properties.

Monte Carlo (MC) method: the Monte Carlo method provides a physical simulation of photon migration. The model assumes a non-deterministic,

stochastic nature for the light scattering and absorption of individual photons.
The required parameters are μ_s', μ_a and $p(\vartheta)$.
Advantages of MC method:
1- The MC method allows a full 3 dimensional description of photon migration;
2- Almost any geometry may be considered;
3- Inhomogeneities can be included;
4- Reflection and refraction may be easily taken into account;
5- The actual scattering properties of scatters can be taken into account.
The main disadvantage is the long computation time required to simulate the motion of a sufficiently large number of photons.

Description of the Monte Carlo (MC) method
Sampling of photon trajectories
Monte Carlo procedures use the probability laws governing photon migration to choose the trajectories of photons. By using a random number generator routine, the trajectories of photons emitted by the source are chosen according to the statistical laws relevant for photon migration through diffusing media. The method makes use of the cumulative probability function $P(x)$:

$$P(x) = \text{probability}(X < x) = \int_0^x p(x')dx' \qquad (0 \le P(x) \le 1)$$

($p(x)$ probability density function) and of a routine generating random numbers (n) uniformly distributed between 0 and 1. The random samples of the variable x are obtained associating to the random number n_i the value of x_i according to:

$$x_i: \; n_i = P(x_i) \qquad \rightarrow \quad x_i = P^{-1}(n_i).$$

We refer to a non-absorbing medium (the effect of absorption can easily be included). From the probability density function relevant for the distance r traveled between two subsequent scattering events ($p(r) = \mu_s \exp(-\mu_s r)$) follows:

$$P(r) = \int_0^r \mu_s \exp(-\mu_s r')dr' = 1 - \exp(-\mu_s r)$$

$$\rightarrow n_i = 1 - \exp(-\mu_s r_i) \quad \text{and} \quad r_i = -\ln(1 - n_i)/\mu_s.$$

The sampling (on the whole solid angle) of the direction along which the photon moves after the scattering event is obtained from two angular distributions for the scattering angle ϑ and the rotation angle φ.

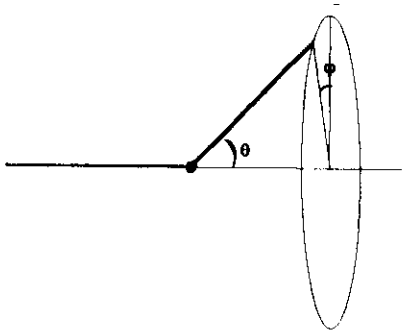

ϑ : scattering angle

φ : rotation angle

$$P(\vartheta) = 2\pi \int_0^{\vartheta} p(\vartheta') \sin(\vartheta') d\vartheta' \rightarrow \quad \vartheta_i : \; n_i = P(\vartheta_i)$$

This relationship is often inverted by using a numerical procedure.

With our assumptions any rotation angle φ has the same probability, therefore:

$$p(\varphi) = 1/2\pi \text{ and } P(\varphi) = \varphi/2\pi \rightarrow \varphi_i : \; n_i = \varphi_i/2\pi \rightarrow \varphi_i = n_i 2\pi$$

By using the rules presented and a routine generating random numbers, the trajectory of any emitted photon is constructed until it exit from the scattering medium or it arrives on the detector.

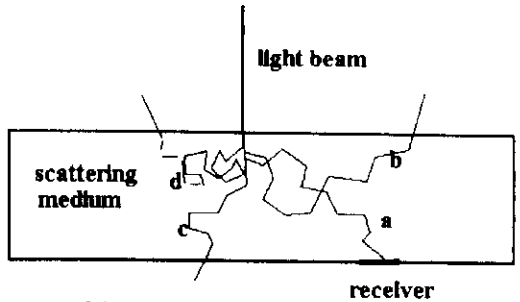

a) useful photon

c, d, b) lost photons

The probability of receiving a photon emitted by the source (i.e., the transmittance) is evaluated as:

$$\frac{N_u = \text{Number of "useful" trajectories}}{N = \text{Number of trajectories considered}}$$

The error on the estimate result is proportional to $1/\sqrt{N}$.

(To simplify the MC scheme, in order to obtain a faster code, the scheme of the random walk approximation is often used to study photon migration in dense scattering media. In this case the MC rules are used to randomly move photons through a discrete cubic lattice).

With MC simulations it is also possible to evaluate the probability that the emitted radiation is received within different temporal windows (i.e., it is possible to evaluate the so called Temporal Point Spread Function (TPSF) $f(t)$) from the histogram obtained classifying the useful trajectories on the base of the length of the trajectory.

Effect of absorption on the TPSF

The TPSF for an absorbing medium can be easily obtained from the TPSF referring to the non-absorbing medium. If $f(t, \mu_a = 0)$ is the TPSF for the non absorbing medium, the TPSF when the absorption coefficient is μ_a, is obtained applying the Lambert-Beer law to any trajectory:

$$f(t, \mu_a) = f(t, \mu_a = 0) \exp(-\mu_a v t)$$

where v is the speed of light in the medium. The total received power when a continuous wave (CW) source is used is given by:

$$P(\mu_a) = P_e \int_0^\infty f(t,\mu_a)dt = P_e \int_0^\infty f(t,\mu_a = 0)\exp(-\mu_a v t)dt$$

where P_e is the power emitted by the source. The equation shows that the total received power is related to the TPSF for the non absorbing medium by the Laplace transform. In principle from measurements of total received power at different values of μ_a it is possible to obtain the same information obtained from measurements in the time domain or in the frequency domain. The TPSF can be obtained by inverting the Laplace transform, in other words $P(\mu_a)$ carries the same information as the TPSF. From attenuation measurements carried out at different values of μ_a by using a simple and inexpensive experimental setup based on a CW source, it is possible to obtain information on the temporal distribution of photons received when the diffusing medium is illuminated by an ultrashort light pulse. As an example, from previous equation it is possible to obtain a simple formula for the mean pathlength, $<l>$, of photons inside the turbid medium:

$$<l> = v <t> = -\frac{d}{d\mu_a}\left[\ln\left(\frac{P(\mu_a)}{P_e}\right)\right] = \frac{P_e v}{P(\mu_a)} \int_0^\infty t f(t,\mu_a)dt.$$

This equation shows that it is possible to determine $<l>$ from measurements with a CW source at two values of μ_a approximating the derivative with the finite differentiation.

OPTICAL PROPERTIES OF BIOLOGICAL TISSUES

Biological tissues are dense packed scattering media. The scattering effect is due to the small differences in the refractive index of different components of cells. The absorption effect is related to the absorption bands of different molecules.

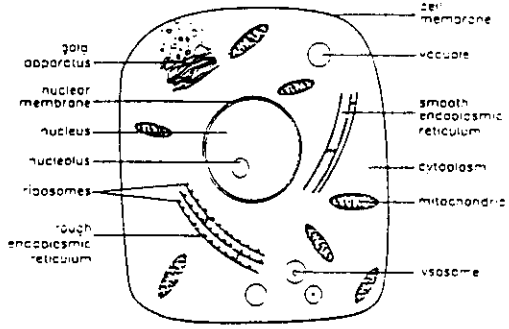

general picture of a cell

Scattering properties of biological tissues at visible and Near infrared (NIR) wavelengths

Since the typical size of cells is usually larger than wavelengths in the visible and NIR range, the scattering properties of tissue slightly depend on λ.

Scattering coefficient

The scattering coefficient of biological tissues at visible and NIR wavelengths is extremely large. As an example, measurements carried out on samples of brain showed $\mu_s \approx 200\,\mathrm{mm}^{-1}$ (corresponding to a mean free path as small as $5\,\mu\mathrm{m}$, i.e., comparable to the wavelength!) for white matter and $\mu_s \approx 20\,\mathrm{mm}^{-1}$ (corresponding to a mean free path as small as $50\,\mu\mathrm{m}$) for grey matter. This means that photons propagating through the tissue undergo very frequent scattering events and follow trajectories similar to random walk.

Scattering function

The scattering function exhibits a highly forward peak, since the typical size of cells is usually large with respect to λ. Typically, more than 50% of the scattered radiation is scattered at $\vartheta < 3°$. The value of the asymmetry factor g is usually close to 1 $(g > 0.9)$.

Reduced scattering coefficient

Typical values measured for μ_s' range from 0.5 to 1.2 mm^{-1}. Therefore, photons migrating through the tissue "forget" the original direction of motion at a penetration depth of the order of 1 mm.

Absorption properties of biological tissues at visible and NIR wavelengths

While the scattering properties slightly depend on the wavelength, the absorption properties are expected to change strongly, since they are related to the absorption spectrum of different molecules constituting the tissue. For biological tissues the absorption properties are often related to the absorption properties of particular groups (called cromophores) within the molecules.
The major absorbing components of many tissues are water, hemoglobin, and melanin. Water ($\approx 70\%$ of the biological tissue) is more or less homogeneously distributed into the tissue, whereas melanin is found mainly in the shin (within few μm) and hemoglobin in the blood. The following figure reports the absorption spectra for these molecules.

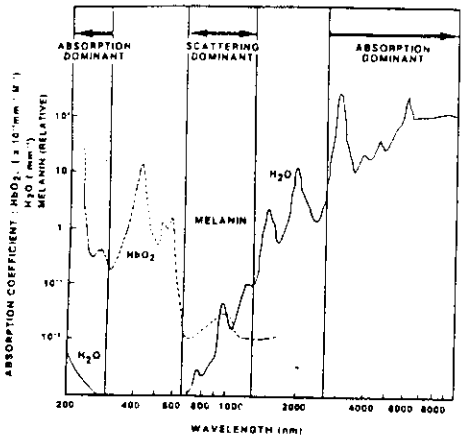

Absorption spectra of water, oxyhemoglobin and melanin.
(Wilson et al., in "Photon migration in tissues" B Chance ed., 1988, Plenum)

The figure shows that the absorption coefficient varies of many orders of magnitude when λ varies within 200 and 10 000 nm. The ranges of λ in which photon migration is dominated by absorption and by scattering are also indicated. Absorption is dominant (the mean free path before absorption is so small that photon migration is simply described by the Lambert-Beer law ($\mu_a \succ 10\mu_s'$)) when $\lambda \prec 300\text{nm}$ or $\lambda \succ 2500\text{nm}$. Radiation at these wavelengths penetrates only a few μm into the tissue before absorption by melanin or by water.

At $650 \prec \lambda \prec 1200\text{nm}$ (scattering dominant region) $\mu_s' \gg \mu_a$ (typical values $\mu_s' \approx 1\,\text{mm}^{-1}$ and $\mu_a \approx 0.01\,\text{mm}^{-1}$) photon migration is well described by the diffusion approximation. Radiation at these wavelengths can follow long trajectories inside the tissue before being absorbed or exiting from the tissue. At these wavelengths radiation can thus penetrate many millimeters before exiting from the tissue (radiation can be detected even after crossing a slab $\approx 10\text{cm}$ thick). Therefore, from this radiation, information can be obtained on the optical properties of deep tissues.

In the following figure we also report the comparison between the absorption spectra of oxygenated and deoxygenated hemoglobin.

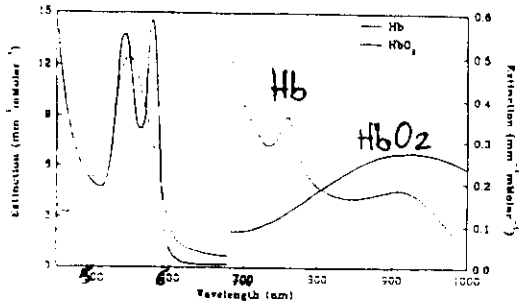

Absorption spectra for oxigenated and deoxigenated haemoglobin (Horecker, J. Biol. Chem., 148, pp. 173, 1943)

The two spectra show significant differences at NIR wavelength, where these cromophores give a substantial contribution to the absorption coefficient. This is reflected in the different color observed for arterial and venous blood. The knowledge of μ_a at two wavelengths enable us to determine the concentration of Hb and HbO_2: a very important parameter, like the tissue oxygenation, can thus be obtained from non-invasive measurements. Usually measurements are carried out at 760 and 800 nm, corresponding to the absorption pick of Hb and to the isosbestic wavelength respectively (at $\lambda = 800\text{nm}$ Hb and HbO_2 have the same absorption coefficient). Many researchers are currently working to develop instrumentation to monitor blood oxygenation.

<u>Problems related to optical monitoring and imaging of biological tissues</u>
The tissue can therefore be monitored studying the diffuse reflectance, i.e., the diffused light emerging from the tissue. However, the study is much complicated by the very large number of scattering events occurring during photon migration: the trajectories of photons received at a few centimeters from the source are very similar to random walks. Thousands of scattering events may occur and photons move along paths that may be very different from the straight line connecting the source and the detector. In these conditions it is difficult to extract information both on the quantization of cromophores responsible of absorption and on the localization of inhomogeneities (tumors, hematomas, etc.) inside the tissue. This occurs because:

1- for the quantitation of cromophores from spectroscopic measurements (measurements of diffuse reflectance at different wavelengths) it is necessary to measure the absorption coefficient (μ_a is proportional to the concentration

of cromophores), but it is impossible to obtain μ_a by using the simple Lambert-Beer law for attenuation: $P / P_e = \exp(-\mu_a L)$, since the effective pathlength followed by the radiation is not known. These difficulties can be overcome if the information on the actual length of the paths followed by received photons is available.

2- the localization of inhomogeneities inside the tissue by using NIR radiation is difficult, since the trajectories of photons may be very different from straight lines and the region of the tissue interested in the migration of photons from the source to the receiver may be very broad. Therefore, scattering effects cause a decrease in contrast and in spatial resolution.

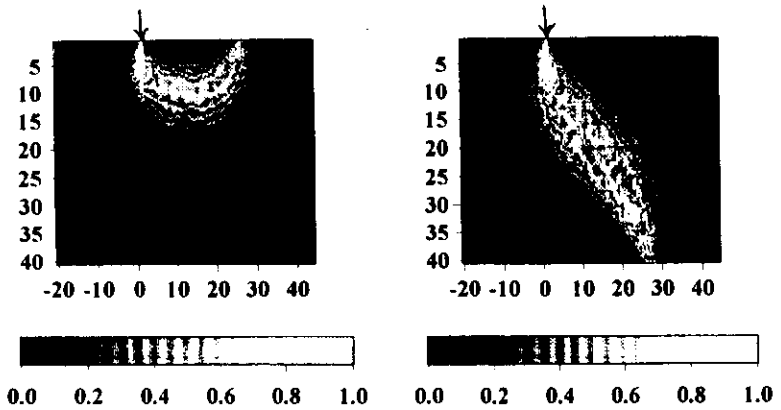

As an example, these figures report the density of scattering points for photons migrating from the source to the receiver. Figures a) and b) refer to a receiver measuring the reflectance and the transmittance respectively, at 25 mm from the light beam. These figures refer to a continuous wave source. The region crossed by received photons is very large. An inhomogoneity inside the turbid medium can significantly alter photon migration (and thus the received signal) also when is placed at a large distance from the straight line connecting the source and the receiver. Data refer to a homogeneous slab of diffusers $40\,mm$ thick with $\mu_s' = 0.5\,mm^{-1}$ and $\mu_a = 0$.

As an example, with a confocal imaging system transilluminating a slab of tissue 5 cm thick (typical value for a breast compressed during x-ray mammography) it is difficult to obtain an image resolution better than about 2-3 cm.

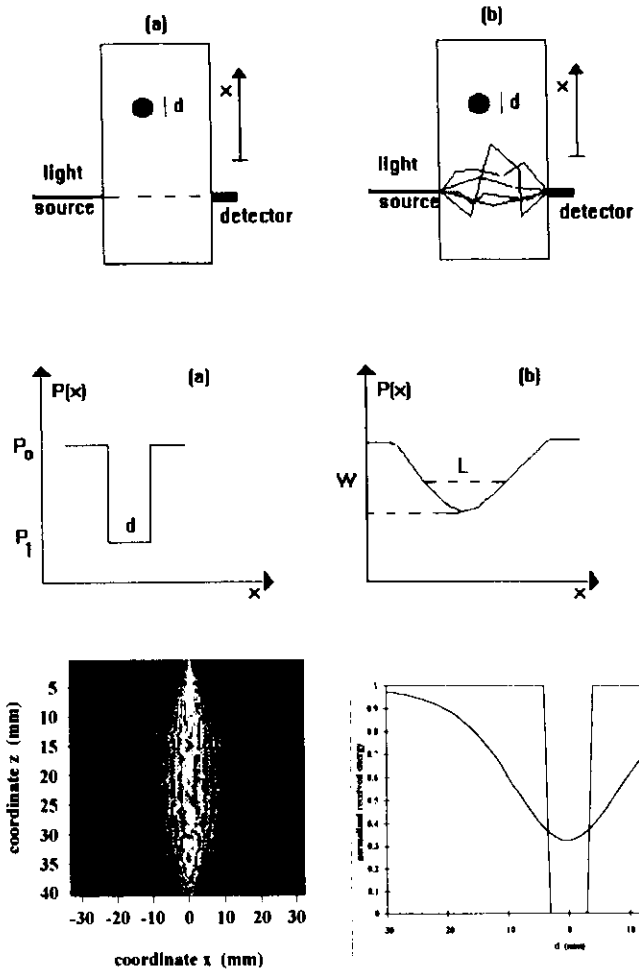

Map representing the density of scattering points for photons migrating from the source to the coaxial receiver. Continuous wave source. Theshadowgram corresponding to a black cilinder (radius 4 mm) placed in the center of the slab is also presented

By using conventional optical techniques (based on CW sources, as diaphanoscopy, studied for a long time for breast imaging), it is thus almost impossible to obtain images of biological tissues having thickness larger than few centimeters, with a quality sufficiently good useful from a medical point of view. Difficulties in image reconstruction can be overcome, and thus the image quality improved, if the information on the actual volume crossed by received photons is available.

Both for optical imaging and for spectroscopy, further information is needed with respect to the one obtained by using conventional techniques based on CW sources. Useful information can be obtained by using recently introduced techniques based on measurements both in the time domain and in the frequency domain.

Measurements in the time domain

Recent progresses on optoelectronics (the availability of light sources emitting ultrashort pulses (picosecond lasers) and ultrafast detectors (streak camera, microchannel plate)) make possible a direct measurement of the temporal spread of a pulse migrating through a biological tissue. An ultrashort pulse (generated by a picosecond lasers) is relayed on the tissue and with an ultrafast detector (a temporal resolution of few picoseconds can be obtained) the time distribution of received photons is measured. The following figures report examples of time resolved measurements carried out on different locations on the same volunteer and on the same organ of different volunteers. (These results were obtained by using the picosecond laser and the streak camera of the LENS (Laboratory for Non Linear Spectroscopy) in Florence). The results refer to measurements of diffuse reflectance measured at 30 mm from the source. Taking into account that the speed of light in biological tissues is $\approx 0.3/1.4\,\mathrm{mm/ps}$ the time necessary to cover the direct source-receiver distance is $\approx 140\,\mathrm{ps}$, the figures show that the mean length of paths followed by photons is 4-7 times larger than the direct path.

Examples of measured TPSF. Interoptode distance 30 mm.

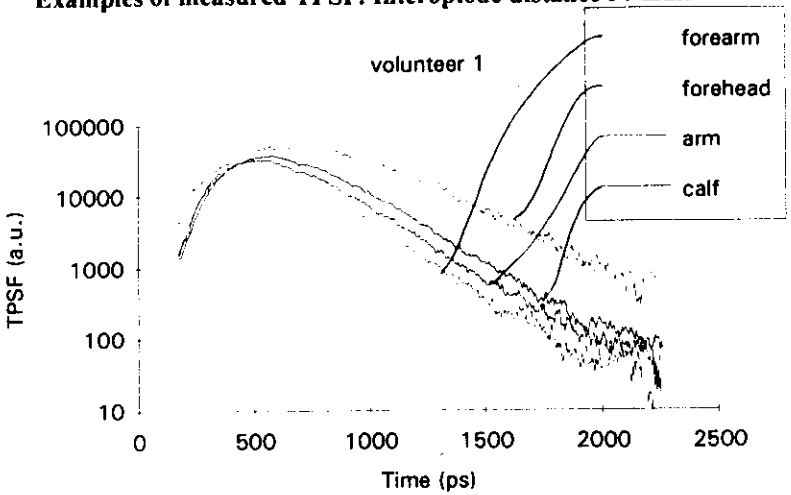

TPSF measured on different organs of the same volunteer.

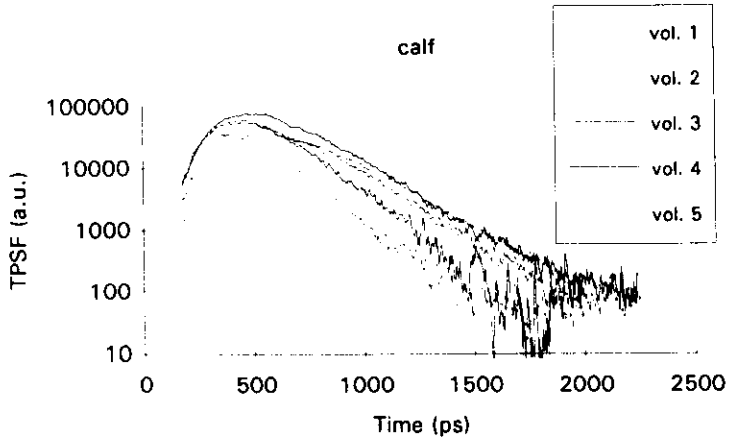

TPSF measured on the same organ on different volunteers.

Experimental setup for time resolved measurements.

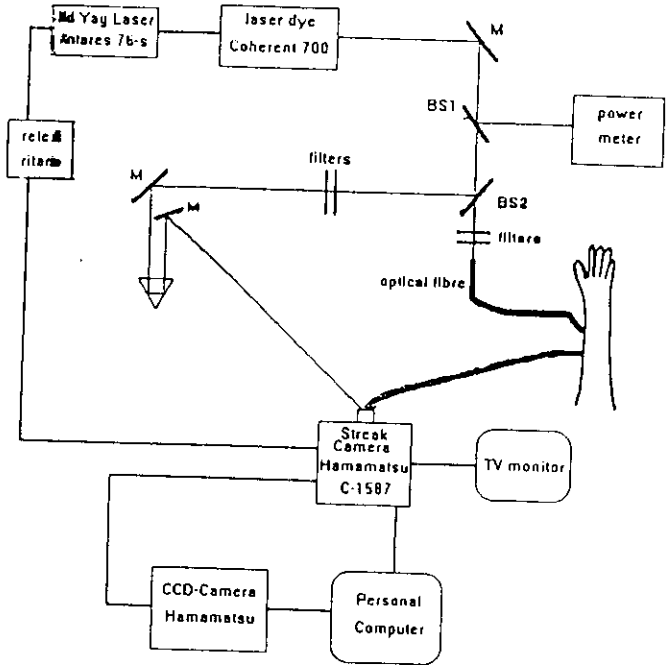

Positioner for optical fifers
(interoptode separation 30 mm)

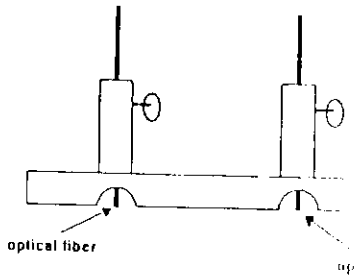

The TPSF depends on μ_a, μ_s' and on the geometrical conditions. If an analitycal model for the TPSF is available, an inversion procedure can be used to obtain μ_a and μ_s' from the measured TPSF. The models currently used for the inversion procedure are derived by using the diffusion approximation.
The next figure shows an example of measured TPSF together with the curve best fitting the experimental results with the model obtained by using the diffusion approximation for a semiinfinite slab of homogeneous diffusers. The values of μ_a and μ_s' obtained from the fitting procedure are also reported in the figure. This example shows how time resolved measurements can be used to determine the absolute value of the absorption coefficient of a strongly diffusing medium. An absolute quantization of different cromophores can be obtained when the value of μ_a is known at different wavelengths.

Example of the inversion procedure: the experimental results are fitted with the formula obtained from the diffusion approximation. The results obtained for the absorption and the reduced scattering coefficient are reported in the following table.

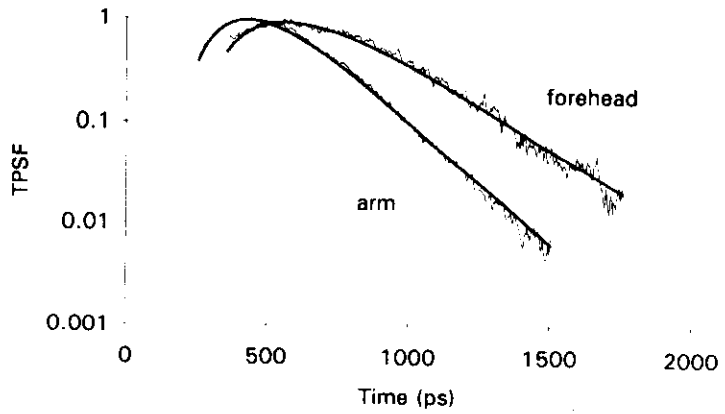

$\lambda = 825\ nm$

	Absorption coefficients (mm-1)			
volunteer No.	arm	forearm	calf	forehead
1	0.0165	0.0208	0.0181	0.0125
2	0.0223	0.0214	0.0217	0.0153
3	0.0223	0.0235	0.0266	0.0153
4	0.0222	0.0252	0.0203	0.0163
5	0.0235	0.0271	0.0275	0.0141

	Reduced scattering coefficients (mm-1)			
volunteer No.	arm	forearm	calf	forehead
1	0.661	0.669	0.851	0.8
2	0.546	0.629	0.764	0.73
3	0.576	0.487	0.679	0.92
4	0.41	0.533	0.588	0.77
5	0.512	0.451	0.511	0.98

Measurements in the frequency domain

Measurements in the time domain require complex and expensive instrumentation. Another approach to obtain information similar to the one obtained from time resolved measurements has been recently proposed. It is based on measurements of the AC and DC component and of the phase of the signal received when the diffusing medium is illuminated by a source emitting a signal with the intensity sinusoidally modulated. The modulation frequencies of interest in tissue optics are between about 40 and 500 MHz. The information obtained in this way is related to the component at the modulation frequency of the Fourier Transform of the TPSF. Therefore the same information can be obtained working in the time or in the frequency domain. The main advantage of the frequency domain approach is the much more simple and less expensive experimental setup.

Also from measurements in the frequency domain it is possible to obtain the value of μ_a and μ_s': a measurement at only one modulation frequency (typically about 100 MHz) is sufficient.

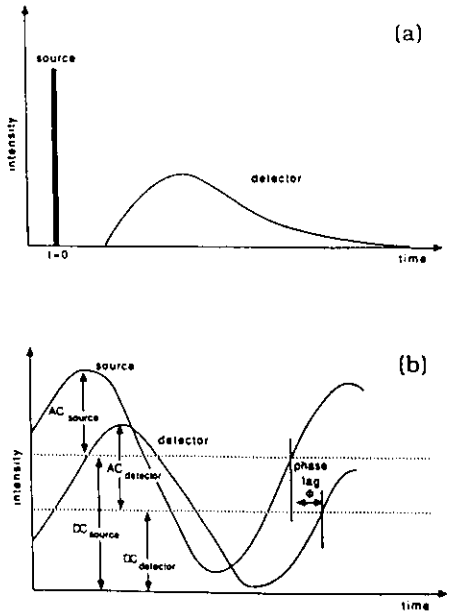

Fig. 1. (a) Schematic representation of the time evolution of the light intensity measured in response to a narrow light pulse traversing an arbitrary distance in a scattering and absorbing medium. If the medium is strongly scattering, there are no unscattered components in the transmitted pulse. (b) Time evolution of the intensity from a sinusoidally intensity-modulated source. The transmitted photon wave retains the same frequency as the incoming wave but is delayed owing to the phase velocity of the wave in the medium. The reduced amplitude of the transmitted wave arises from attenuation related to scattering and absorption processes. The demodulation is the ratio ac/dc normalized to the modulation of the source.

Fishkin and Gratton, JOSA A, 10 pp. 129 (1993)

Techniques for imaging of biological tissues by using visible and NIR radiation

The localization of inhomogeneities inside the tissue by using NIR radiation is difficult, since the trajectories of photons may be very different from straight lines and the region of the tissue interested in the migration of photons from the source to the receiver may be very broad. An improvement in contrast and spatial resolution can be obtained by using two different approaches:

1- Time gating techniques.

These techniques, investigated especially for breast imaging, are based on measurements of time resolved transmittance. They involve discriminating between few marginally deviated photons and all other scattered light, measuring the time-of-flight of the transmitted photons.

EXAMPLES OF MAPS REPRESENTING THE DENSITY OF SCATTERING POINTS FOR PHOTONS RECEIVED WITHIN DIFFERENT GATING TIMES (Δt_g) FROM A RECEIVER COAXIAL WITH THE LIGHT BEAM. $\tau_s' = 20$

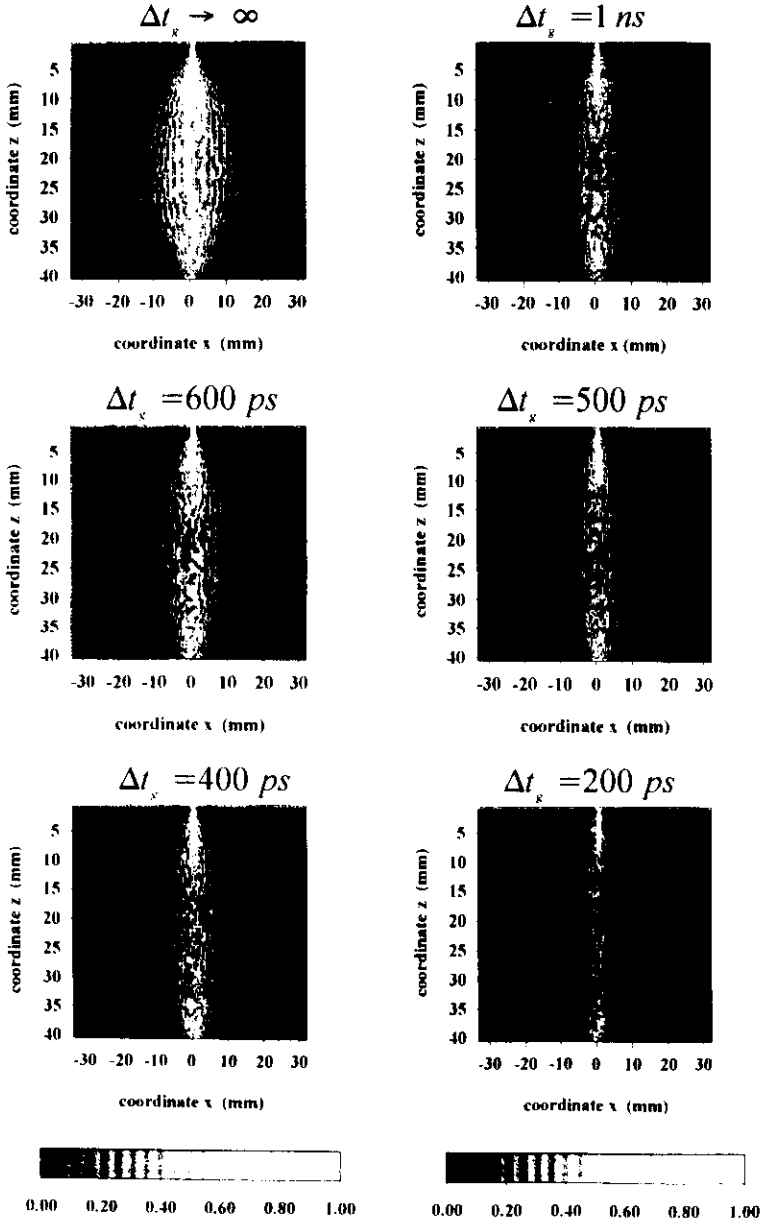

EXAMPLE OF SHADOWGRAMS OBTAINED MOVING THE SOURCE-RECEIVER SYSTEM ACROSS THE BLACK CYLINDER (DIAMETER 6mm): NUMERICAL RESULTS. $\tau_s' = 20$

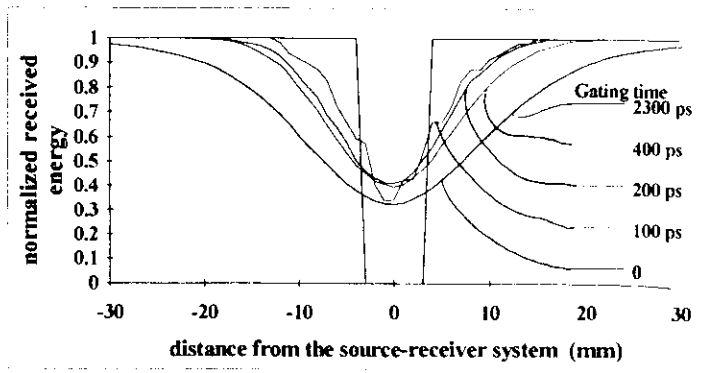

Different curves refer to different gating times.

When the gating time decreases the shadowgram becomes narrower and thus the image resolution increases. However, the contrast (related to the ratio betveen the maximum and the minimum of the shadowgram) increases only when very short gating times are considered.

With the time-gating technique the image reconstruction involves only earlier detected photons that are the least deviated from the laser beam axis. In this way, it is possible to limit the image blurring, recovering contrast and spatial resolution. The spatial resolution obtainable with this method is ultimately limited by the strong attenuation of energy received during short gating times. When unscattered (ballistic) photons can be detected a high quality image can be obtained. However, for strong scattering media like biological tissues, it becomes almost impossible to measure the received energy when the gating time becomes very short. Recent studies have shown that the spatial resolution obtainable in typical physical and geometrical conditions for breast imaging is not better than one centimeter. A method to further improve the spatial resolution was recently proposed. This method involves the use of all information carried by TPSF: experimental results were fitted with an analytical model for the TPSF. A spatial resolution of about 5 mm was obtained by using the signal corresponding to very short (20 ps) gating times inferred from the analytical model.

1a)- Another possibility to discriminate the few marginally deviated photons, without the need for time resolved measurements, is to carry out

measurements in presence of a strong absorption. Photons that undergo many scattering events, travelling long trajectories in a purely scattering medium, are strongly reduced when the absorption effect is introduced. An improvement in image quality, similar to the one obtained by using short gating times, is thus expected when attenuation measurements of a continuous wave (CW) source are carried out at high absorption coefficients. Next figure reports examples of TPSF evaluated with a Monte Carlo simulation for different values of μ_a: when μ_a increases the received power decreases, but also <I >decreases.

EFFECT OF ABSORPTION ON PHOTON MIGRATION: NUMERICAL RESULTS

When the absorption coefficient is increased the received intensity is decreased, but the TPSF is strongly shortened. $\tau_s' = 20$

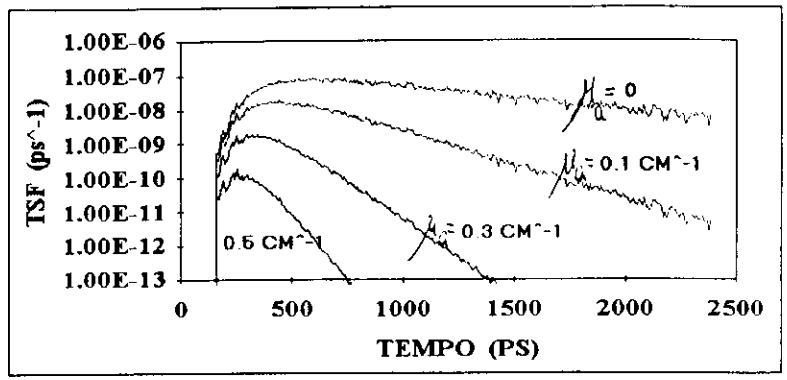

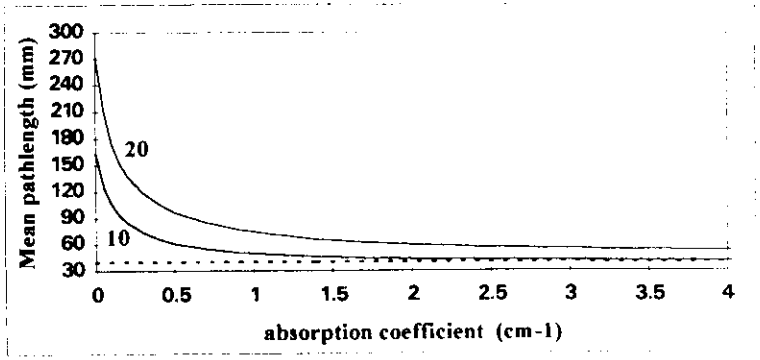

$\tau_s' = 10$ e $\tau_s' = 20$

These figures refer to the signal transmitted through a slab of homogeneous diffusers and received by a detector (radius = 5 mm) coaxial with the thin light source. The slab is 40 mm thick, the reduced scattering coefficient $\mu_s' = 0.5\ mm^{-1}$, the asymmetry factor g = 0 and the refractive index n = 1.

MAPS REPRESENTING THE DENSITY OF SCATTERING POINTS FOR PHOTONS MIGRATING FROM THE SOURCE TO THE RECEIVER: EFFECT OF ABSORPTION. $\tau_s' = 20$

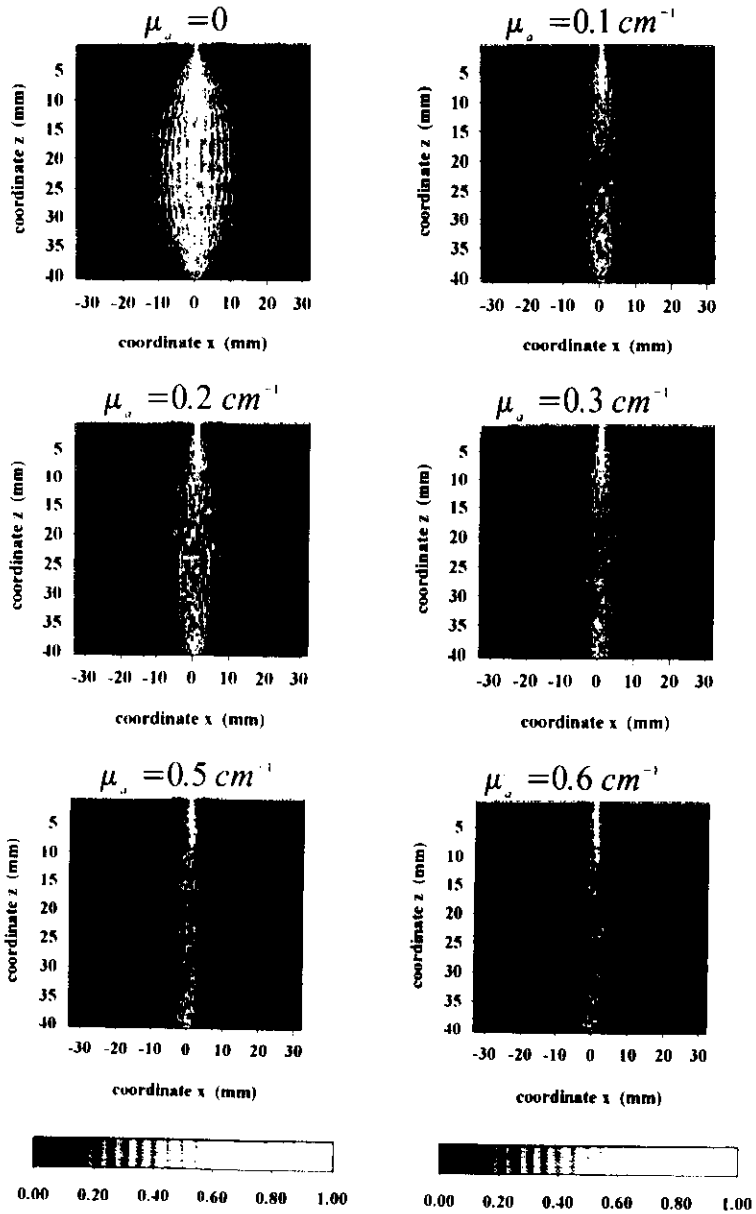

MAPS OF SCATTERING POINTS FOR COMPARISON BETWEEN TIME-GATING TECHNIQUE AND ABSORPTION METHOD

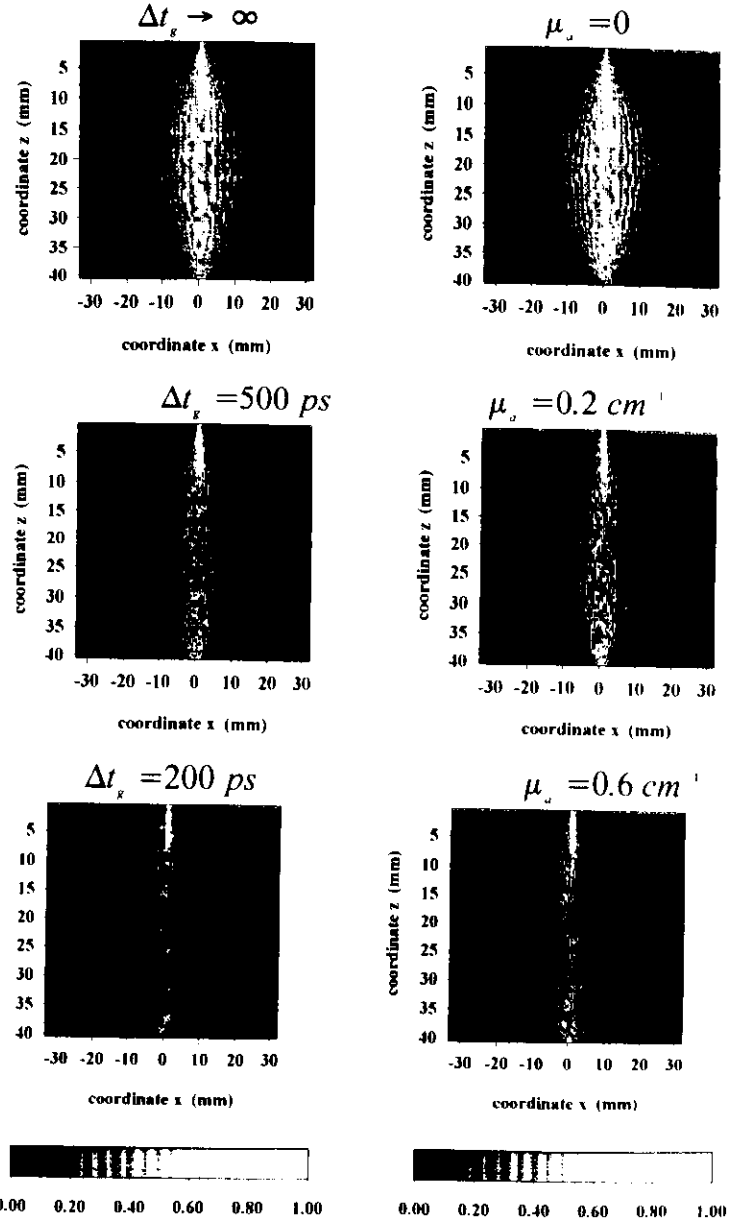

Similar effects are obtained increasing μ_a or decreasing the gating time

Also for the absorption method the spatial resolution obtainable is ultimately limited by the strong attenuation of energy received when a strong absorption effect is present.

2- Optical tomography. Another possibility to improve the spatial resolution and the localization of the inhomogeneity is given by tomographic measurements.
To illustrate the problem of optical tomography we refer to the following figures, reporting the density of scattering points for photons received within different temporal windows.

The following figure shows examples of maps representing the density of scattering points for the trajectories of photons received within three different temporal windows: 0-600 ps, 600-1400 ps, and 1400-5800 ps from upper to lower panels, respectively (within 5800 ps practically all received photons reach the receivers). Left and right panels refer to photons received at the detector measuring the reflectance and the transmittance, respectively. The area of the receivers, placed at a distance of 26 mm from the light beam, was 24 mm^2. These maps show the region of the diffusing medium through which photons received within different temporal windows pass during migration from the source to the receiver. These maps were obtained by projecting the scattering points on the *xz* plane and assuming a grey level proportional to the density of scattering points.

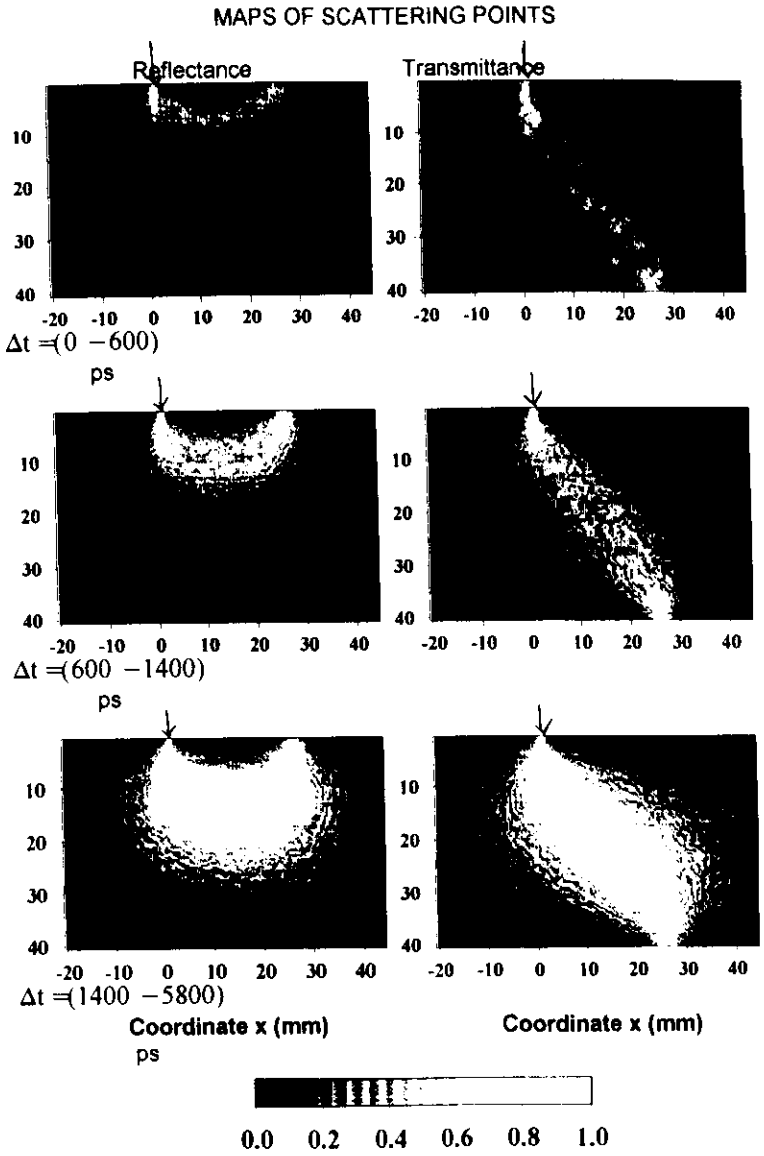

Maps representing the density of scattering points for different temporal windows. These maps show the region of the diffusing medium through which photons received within different temporal windows pass during migration from the source to the receiver.

L = 40 mm; $\mu_s' = 0.5\ mm^{-1}$; $\mu_a = 0$; n = 1.33.

Data presented in the previous figure refer to a homogeneous slab of diffusers $40\,mm$ thick with $\mu_s' = 0.5\,mm^{-1}$ and $\mu_a = 0$. The value $0.225\,mm/ps$ was assumed for the speed of light into the medium. The figure shows that photons arriving within shorter transit times (i.e., the ones having undergone a smaller number of scattering events) have a smaller probability to deviate significantly from the line connecting the source and the receiver. The region crossed by photon migration becomes larger and larger when the transit time increases. As an example, the figure shows that for photons received at the detector measuring the reflectance the probability to reach a distance greater than about 15 mm from the middle point between the source and the receiver is very small for early photons, whereas there is a significant probability for photons arriving within 1400 and 5800 ps to reach distances as large as 35 mm. Therefore photons arriving within different temporal windows carry information on the optical properties of different regions of the diffusing medium.

Time resolved measurements give us the possibility to discriminate between photons passing through different regions of the medium. The big problem for optical tomography is "how" to use the information content of the TPSF, i.e., the inverse problem. There are currently many efforts to develope efficient reconstruction algorithms. The starting point for these algorithms is a correct model describing the probability that photons received within any temporal window have passed through different volume elements of the medium, i.e., a correct understanding of photon migration through dense diffusing media.

In the scheme followed to illustrate photon migration through tissues we considered only the elastic scattering effect and we have not discussed about the radiation absorbed by the tissue. There are different mechanisms, responsible both for absorption and for decaying depending on the particular molecule and on wavelength of the exciting light, from which further information can be obtained.